Air Flows along Perforated Metal Plates with the Heat Transfer

K. Fraňa, S. Simon

Abstract—The objective of the paper is a numerical study of heat transfer between perforated metal plates and the surrounding air flows. Different perforation structures can nowadays be found in various industrial products. Besides improving the mechanical properties, the perforations can intensify the heat transfer as well. The heat transfer coefficient depends on a wide range of parameters such as type of perforation, size, shape, flow properties of the surrounding air etc. The paper was focused on three different perforation structures which have been investigated from the point of the view of the production in the previous studies. To determine the heat coefficients and the Nusselt numbers, the numerical simulation approach was adopted. The calculations were performed using the OpenFOAM software. The three-dimensional, unstable, turbulent and incompressible air flow around the perforated surface metal plate was considered.

Keywords—Perforations, convective heat transfers, turbulent flows, numerical simulations.

I. INTRODUCTION

PERFORATED metal plates can be found in different technical applications from civil engineering up to mechanical engineering and particularly, in the automotive industry. For instance, Fig. 1 shows the perforated metal sheet used in a vehicle. The task of the metal plates was to reduce or even prevent the spreading of heat from the exhaust gases into the inside of the car.
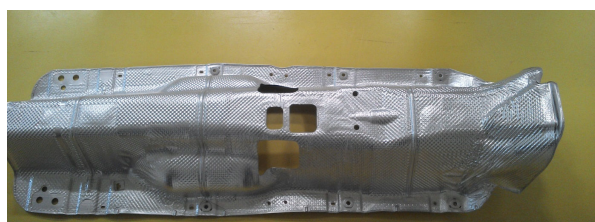

Fig. 1 Perforated metal plates used in the car engine

The company Mercedes uses such sheet metals at various parts of the car SLK. Fig. 2 depicts how the different materials with structured surfaces are used in the car production. In residential or non-residential buildings and houses, structured metal sheets can be also found in cake tins. As in the automotive industry, it provides the intensive thermal

K.Fraňa is with the Technical university of Liberec, Department of Power Engineering Equipment, 461 17, Liberec, Czech Republic (phone: +420 48 535 3436; fax: +420 48 535 3434; e-mail: karel.frana@seznam.cz).

S.Simon is with the Brandenburgische Technische Universität Cottbus – Senftenberg, 01968 Senftenberg, Großenhainer Str. 57, Germany, (phone: 03573 85 -425; -404; e-mail: sylvio.simon@b-tu.de).

conduction over the entire surface. Another application of perforated metal plates is in washing machines. Besides thermal properties, the perforation can improve the mechanical properties as well. The perforations cause a greater moment of inertia due to the appropriate structures than the classical plain metal sheets. Simultaneously, they also have a higher bending stiffness than a plain sheet with the same sheet-thickness.
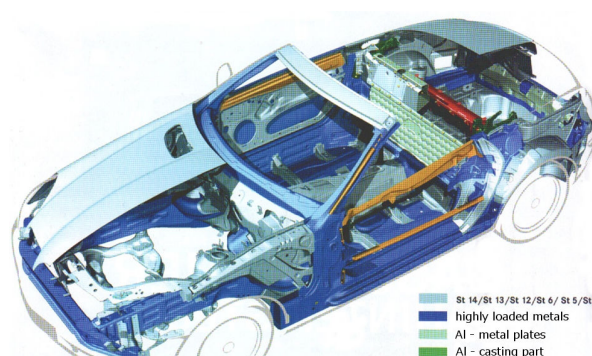

Fig. 2 Variety of the material uses in the car design

TABLE I
STRUCTURE HEIGHT AND FORMING PRESSURES ARE COMPARED FOR ALUMINUM ALLOY AA 5052-O AND DEEP-DRAW STEEL PRODUCED BY DIFFERENT STRUCTURING PROCESSES

Manufacturing process	Structure		Height (mm)	Applied Pressure (N/mm2)
Rolling	Aluminum Alloy, AA 5052-0		2,15	3,69
	Deep-Draw Steel		1,8	3,32
Rolling	Aluminum Alloy, AA 5052-0		2,4	6,16
	Deep-Draw Steel		-	-
Rolling	Aluminum Alloy, AA 5052-0		1,6	3,46
	Deep-Draw Steel		1,6	5,39
Hydro-forming	Aluminum Alloy, AA 5052-0		1,6	3,46
	Deep-Draw Steel		1,4	4,46
Vault structured	Aluminum Alloy, AA 5052-0		3,1	0,23
	Deep-Draw Steel		3,1	0,23

The mechanical properties of a structured metal sheet depend on the shape of the structures, separations and the

World Academy of Science, Engineering and Technology
International Journal of Mechanical and Mechatronics Engineering
Vol:9, No:8, 2015

height (size). Through the perforations, the elasticity increases into the direction of pull, however, the axial rigidity decreases. Therefore, in production, the perforated metal plates are easily crafted into complex forms like the exhaust channel (see Fig. 1). Structured sheet metals can be crafted using warping, rolling or hydroforming process (see Table I). If a sheet is crafted by the rolling process the structural roller has to circulate synchronously. It causes a displacement of the structure leading to a change of the mechanical properties of the sheets. Due to the structural procedures, strain hardening is obtained and simultaneously, different thicknesses can be observed [1]. The Vault-structuring method shows the capability to form relatively high structures at low forming pressures [2].

Besides the mechanical properties, the perforation of the metal plates can increase the thermal properties as well. This fact can be well illustrated in a wide range of publications [3]-[5]. Generally, the perforated surfaces close to the air flow initiate fluid flow fluctuation and therefore it can increase the heat transfer coefficient between the surface and surrounding flows due to intensified mixing. It is well known from thermodynamic theory, that the turbulent boundary layer has a higher coefficient for convection heat transfer than a plain metal under the same flow and temperature conditions. Dutta et al. [6] investigated experimentally the effect of baffle size, perforation, and orientation on internal heat transfer enhancement. Two parameters are used for result evaluation; the Nusselt number and a friction parameter. Generally, the perforated density, position, and size of the baffles have a significant effect on the internal heat transfer. The friction factor ratio decreases with an increase in the perforation density. The average Nusselt number ratio mostly stays at a fixed value with different Reynolds number for a given baffle plate. A similar subject of investigation is introduced in this paper. In order to recommend the appropriate metal plate perforation in regards to the heat transfer, the computational fluid dynamics (CFD) approach is adopted for the investigations. The idea of the numerical simulations with particular boundary condition prescriptions is explained in the chapter "Problem formulation". The chapter "Results" shows and discusses flow features and heat transfer mechanisms which play a significant role in the heat transfer intensity from the metal surface plate to the surroundings. The chapter "Conclusion" summarized significant findings and heat transfer phenomena discovered.
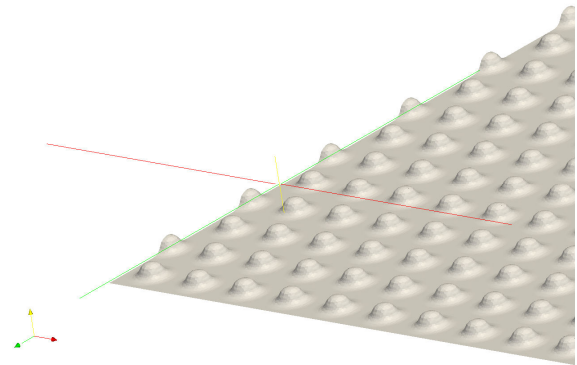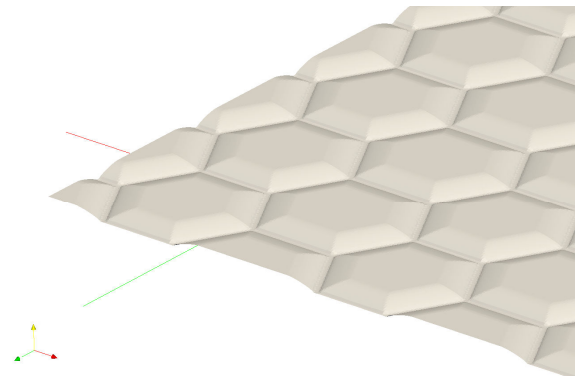

Fig. 3 Ledge shape of perforation (pattern1)

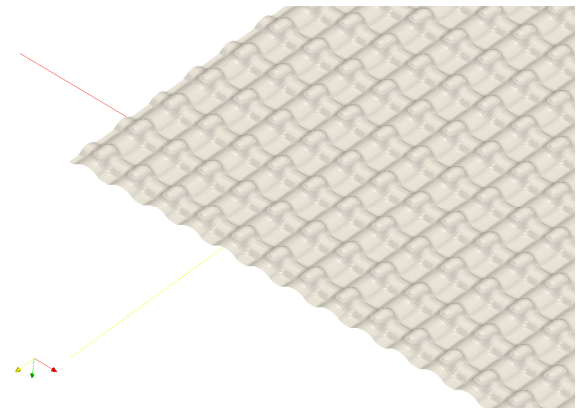Fig. 4 Perforation of a hexagonal shape (pattern2)

Fig. 5 Non-uniform Sinus form shape of the perforation (pattern3)

II. PROBLEM FORMULATION

Three different types of perforations are considered in this study in order to determine the heat coefficients in the convective heat transfer. Figs. 3-5 illustrate the shapes and size of the perforations which represents the ledges, hexagons, or sinus forms. Fig. 6 shows a computational domain with boundary condition prescriptions and with the perforated surface of the metal plate. The air flow orientation is depicted by the yellow arrow with a velocity intensity of 1 m/s at the inlet and at the moving wall, respectively. The turbulent properties are defined by the turbulence intensity. The size of

World Academy of Science, Engineering and Technology
International Journal of Mechanical and Mechatronics Engineering
Vol:9, No:8, 2015

the computational domain is almost 240x240x20m for all the investigated patterns. This size of domain was suggested in regard to the density of the perforation. The second aspect was the possibility to generate a computational grid with higher sensitivity to resolve the perforation details. The Reynolds number based on the metal plate length is of $2,4x10^7$. Therefore, the flow was considered as three dimensional, unstable, incompressible, and turbulent. The turbulence was treated numerically by the RANS turbulence model k-epsilon Standard [7]. This model provides mostly satisfactory flow results at higher Reynolds numbers. It is commonly used in industrial applications because of its robustness [7]. The surface temperature is isothermal and its value is 60°C and the temperature of the inlet air flow is 20°C. The heat transfer was carried out by force convection between the metal plate surface and the surrounding flowing air. The total heat transfer is defined as

$$Q = \dot{m}c_p\left(t_{out} - t_{in}\right), \tag{1}$$

where ṁ indicates the air flow rate, c_p is the specific heat capacity under constant pressure and t is the temperature at the inlet and outlet. The heat coefficient for the convective heat transfer can be found from (2):

$$Q = \alpha(t - t_s)S \tag{2}$$

In (2), α is the coefficient for the heat convection, t is the average temperature in the air flow, t_s is the temperature at the surface of the plate and S is the surface area. The heat transfer can be characterized by the non-dimensional parameter Nusselt number which takes the form as

$$Nu = \frac{\alpha\, l}{\lambda}, \tag{3}$$

where l is the length scale and λ is the heat conductivity coefficient. Furthermore, the Boussinesq approach was assumed for the heat transfer calculation. This calculation gives satisfactory results under conditions if the temperature difference is in the order of units.
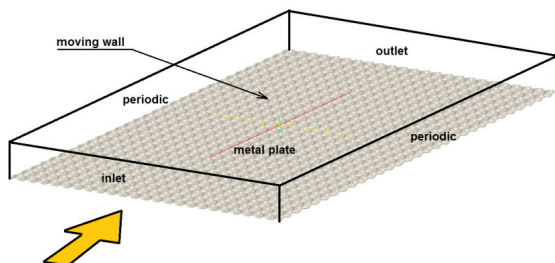

Fig. 6 Sketch of model with definitions of the boundary conditions

The computational grid was generated by the SnappyHexMesh grid generator. The SnappyHexMesh tool

provides instruments to generate a computational grid in a domain created by cutting a preliminary mesh block according to the shape of the surfaces.

Fig. 7 the area colored red will be extracted from the grey mesh block. Fig. 8 shows computational grid after extraction but before the surface grid refinement. Fig. 9 depicts the final refined surface grid which takes the form of the real perforations considered in the study.
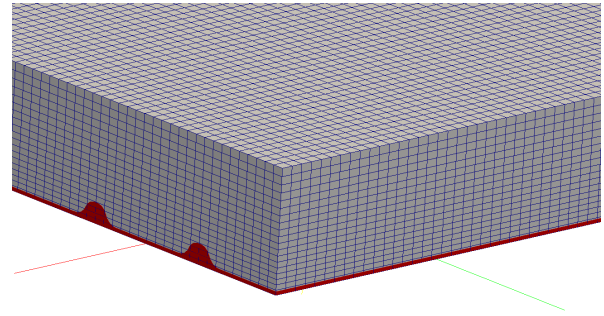

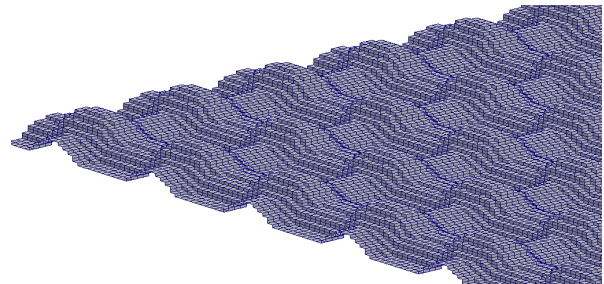Fig. 7 The computational grid before surface extraction

Fig. 8 Surface mesh before grid refinement

The computational grid used in the flow study contained approximately 1,8 million cells mostly of the hexahedral type. The grid quality was described by a maximal (6,46) and minimal cell volume (0,0071). The maximal skewness was 2,47 and maximal aspect ratio was 8,13. The numerical simulation was carried out using OpeanFOAM calculations. The flow over a plate involves, generally, laminar, turbulent or mixed boundary layer assumptions.
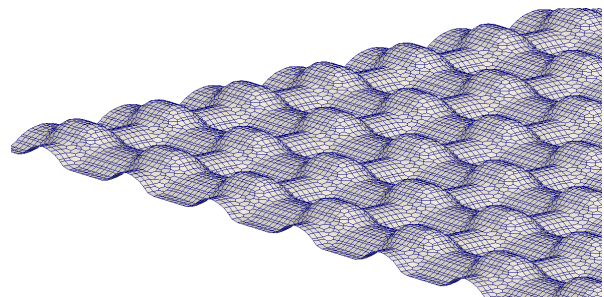

Fig. 9 Surface mesh after grid smoothing

The theory of mixed boundary layer conditions is mostly adopted for the averaged Nusselt number or friction coefficient calculations [8]. The Nusselt number is defined as

World Academy of Science, Engineering and Technology
International Journal of Mechanical and Mechatronics Engineering
Vol:9, No:8, 2015

$$Nu_L = (0{,}037\,\mathrm{Re}_L^{4/5} - A)\,\mathrm{Pr}^{1/3} \qquad (4)$$

where parameter A is defined as

$$A = 0{,}037\,\mathrm{Re}_{xc}^{4/5} - 0.664\,\mathrm{Re}_{xc}^{1/2} \qquad (5)$$

The Reynolds number Re_{xc} is based on the length indicating a threshold between laminar and turbulent boundary areas. In the case that only a turbulent boundary condition is assumed, the Nusselt number definition takes the form of

$$Nu_L = 0{,}0296\,\mathrm{Re}_L^{4/5}\,\mathrm{Pr}^{1/3} \qquad (6)$$

The Prandtl number should be between the values of 0,6 and 60. The velocity boundary layer thickness may be expressed as

$$\delta = 0{,}37\,\mathrm{Re}_L^{-1/5} \qquad (7)$$

In the frame of the current study, the turbulent boundary type layer is assumed for the entire domain. The theoretically calculated Nusselt number for the plain surface without any perforations was 21207. The calculation of the Nusselt number from the CFD was significantly higher, approximately $N_{u0}=41370$. It is further used as a reference value for the heat transfer evaluations. Another parameter used for the evaluation of the metal plate perforations is a friction parameter. It involved the effect of the pressure drop along the length of the metal plate. The equation defining the friction coefficient takes a form of

$$C_f = \frac{\Delta p h}{\frac{1}{2}\rho L V^2} \qquad (8)$$

where Δp indicates a pressure drop, h is the height of the computational domain, L is the characteristic length scale, V is the average velocity and ρ is the density. Assuming only plain metal without any perforations, the average friction coefficient is calculated as

$$C_f = 0{,}0592\,\mathrm{Re}_L^{-1/5} \qquad (9)$$

This equation is valid for turbulent flows up to the Reynolds number of 10^8. For the plain metal plate considered in this study, the friction coefficient reaches the value of 0,002. The calculated value of the friction parameter using the CFD was 0,006.

III. RESULTS

Figs. 10-12 illustrate the time average temperature field in the slice extracted close to the outflow boundary conditions. The temperature values are scaled by the temperature at the inlet condition. The temperature field is non-uniform in the entire computational domain characterized by the higher and lower temperature regions. These areas vary periodically depending on how the perpendicularly oriented air flow declines or inclines to or from the structured surface. In practice, if the air flow declination appears at the surface, the air with higher temperature started to flow into the surrounding area leading to an increase of temperature.
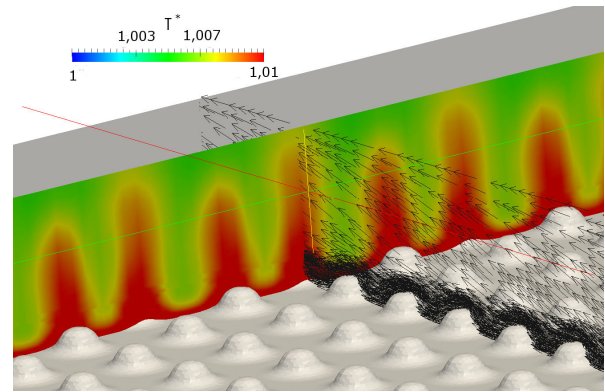

Fig. 10 The time average temperature field in the slice perpendicular to the flow stream for metal plate pattern 1
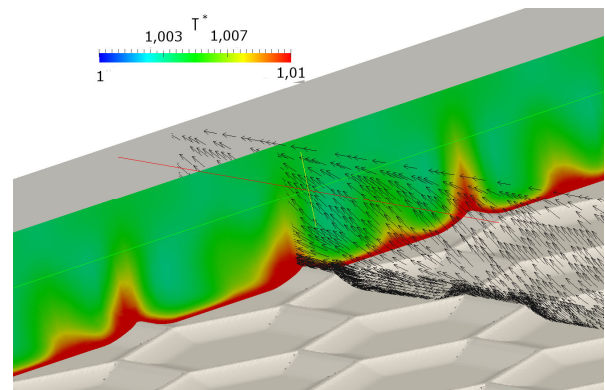

Fig. 11 The time average temperature field in the slice perpendicular to the flow stream for metal plate pattern 2
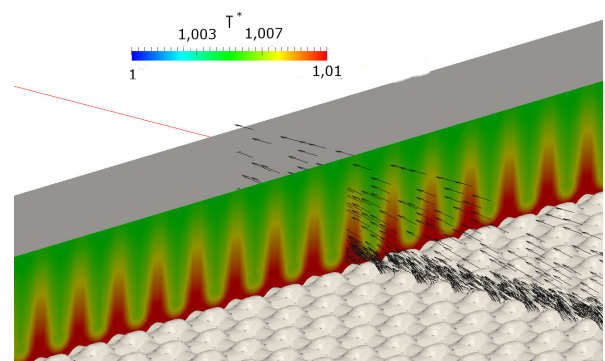

Fig. 12 The time average temperature field in the slice perpendicular to the flow stream for metal plate pattern 3

From the point of the heat transfer, these phenomena can be interpreted as the intensification of the convective heat transfer coefficient. Fig. 10 demonstrates this effect well. It shows the

World Academy of Science, Engineering and Technology
International Journal of Mechanical and Mechatronics Engineering
Vol:9, No:8, 2015

air flow depicted by the black vectors and the temperature distribution in the slice perpendicular to this flow. The air flow is oriented from the surface due to surface perforations. The same effect can be identified in Figs. 11 and 12 as well. Of course, the structure determines the final flow features and therefore, the temperature distribution in the surrounding area of the perforated metal plates. Simultaneously, this flow phenomena described influences the velocity distribution at the same slice. The maxima and minima of the air velocity flow were detected depending on how the character of the air flow was deformed by the structure shapes (depicted by vector representations with black color).
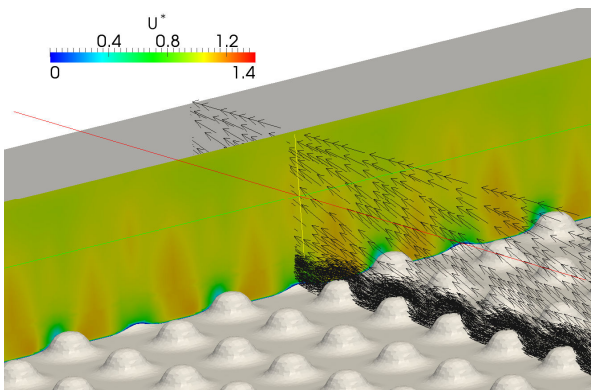

Fig. 15 The time average velocity field in the slice perpendicular to the flow stream for metal plate pattern 3
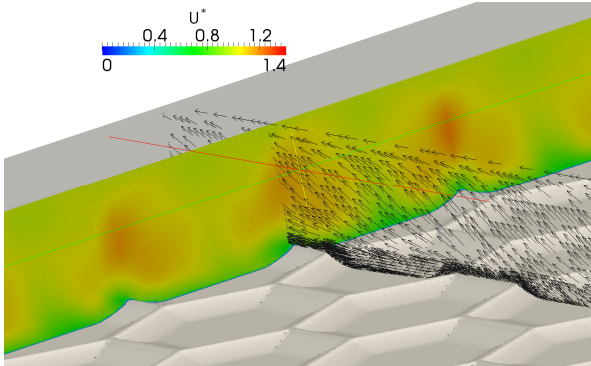

Fig. 13 The time average velocity field in the slice perpendicular to the flow stream for metal plate pattern 1

Fig. 16 Pathlines of the air flow along the perforated surface plate for pattern 1

Fig. 14 The time average velocity field in the slice perpendicular to the flow stream for metal plate pattern 2

Fig. 17 Pathlines of the air flow along the perforated surface plate for pattern 2

Different patterns are well demonstrated in Figs. 13-15. The velocity value is scaled by the air velocity at the inlet. Figs. 16-18 show path lines over the perforated metal plate. The color indicates the air velocity intensity scaled by the velocity of air at the inlet. At the same position along the main flow, the air stream declines from the surface (depending on the perforations and positions) which leads to an increased rate of heat transfer. In particular, it improves the mixture of the cold and hot air and therefore it increase the convective heat transfer coefficient.
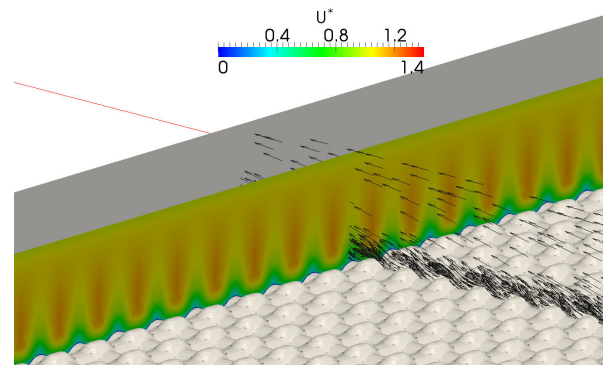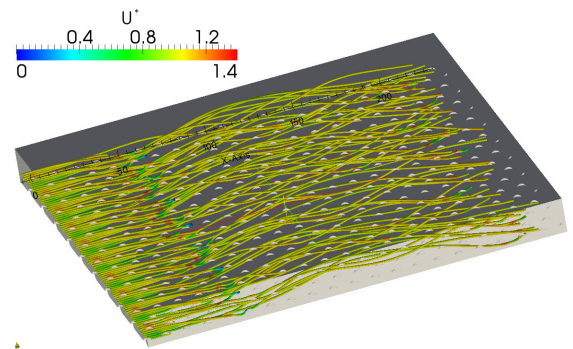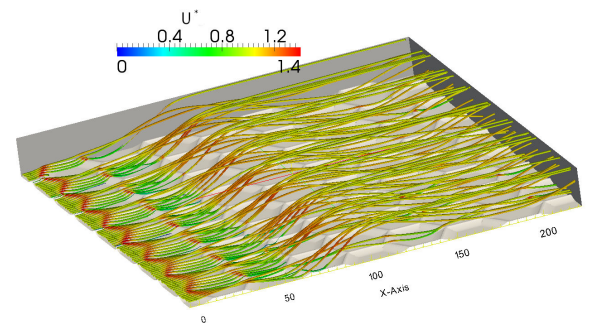
The visualization of the pathlines revealed that the effect of the declining flow appered intensively in pattern 1 and less in pattern 2. Furthermore, the declined air flow in pattern 2 had a tendency to incline back to the perforated surface. This observation is a good match with the results of the calculated heat transfer coeffcients and Nusselt numbers.

Table II summarizes the heat transfer coefficients and Nusellt numbers calculated by the numerical results. Pattern 1 demonstrated about 6% higher heat transfer than the numerically calculated one for the plain surface (without any perforation and rouhgness).
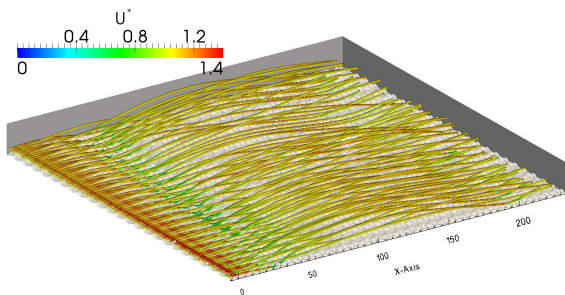
World Academy of Science, Engineering and Technology
International Journal of Mechanical and Mechatronics Engineering
Vol:9, No:8, 2015

Fig. 18 Pathlines of the air flow along the perforated surface plate for pattern 3

TABLE II
HEAT TRANSFER FOR PERFORATED METAL PLATES

	T_{in}	T_{out}	V	a	Nu_{avg}	Nu_{avg}/Nu_0
	[K]	[K]	[m3/s]	[W/m^{2}K]		
1	293	295,6	4653	4,71	43984	1,063
2	293	294,8	5380	5,123	47841	1,156
3	293	295,4	4708	5,268	49193	1,189

Pattern 2 can provide about 15% higher value of the Nusselt number than can exist on a plain wall. The higher value of Nusselt number was found for pattern 3, with about 19% higher heat transfer intensity. Of course, the same conclusion can be found for the heat transfer coefficients. It is important to take into account that these Nusselt number values for all three patterns were calculated for the particular Reynolds number, size of the perforation and temperature difference.

TABLE III
PRESSURE DROP AND FRICTION COEFFICIENT FOR PERFORATED METAL PLATES

	p_{in} (Pa)	p_{out} (Pa)	C_f	C_f/C_{f0}
1	99,588	90,202	0,064	10,6
2	97,68	97,42	0,043	7,2
3	88,59	87,81	0,13	21,7

The calculation of the friction coefficient was carried out using the formula given by the definition in (8) and it is summarized in Table III. Pattern 3 significantly revealed the highest pressure drop. The lowest pressure drop was identified for pattern 2. Considering the magnitude of the friction coefficient, generally for all investigated patterns, it is up to 1 order higher than it would be on a plain wall.

IV. CONCLUSION

This paper presented a flow study of how the convective heat transfer appeared between perforated surfaces and the air flow in the surroundings. The CFD approach was adopted to confirm the assumption that perforations can improve heat transfer. It was used furthermore to precisely specify the values of the heat transfer and friction coefficients for three commonly used perforations. The numerical calculations provided results of the instantaneous and time average velocity fields, temperature and pressure distribution under the influence of the surface perforations. Assuming two criterions

for the evaluation of the results, the friction coefficients and the heat transfer coefficient were used. The comparison between theoretical and numerically calculated values showed a difference of a factor of 2 for the heat transfer and a factor of 3 for the friction parameter. The pattern number 3 reached the highest Nusselt numbers reaching up to 19% higher value than in the plain plate. However, the friction coefficient was 21,7 times higher than for the plain wall. Pattern 2 provided about 16% higher heat transfer coefficient than for the plain wall. Simultaneously, the friction parameter was higher only about 7%. Pattern 2 is the best choice in respect of the optimal combination of the heat transfer and friction coefficients.

REFERENCES

[1] S. Simon, *Werkstoffgerechtes Konstruieren und Gestalten mit metallischen Werkstoffe*, Verlag Dissertation.de, ISBN 978-3-86624-324-8, 2008
[2] M. Hoppe, *Umformverhalten strukturierter Feinbleche*, "Diss. Brandenburgische Technische Universität (BTU), Cottbus, 2003
[3] T. Kuppan, Heat exchanger design handbook, CRC Press, 2000.
[4] S. Kakaç, A.E. Bergles, F. Mayinger, H. Yüncü, *Heat transfer enhancement of heat exchangers*, Kluwer, 1999.
[5] A. D. Kraus, A. Aziz, J. Welty, *Extended surface heat transfer*, John Wiley & Sons, 2001.
[6] P. Dutta, S. Dutta, Effect of baffle size, perforation, and orientation on internal heat transfer enhancement, *International Journal of Heat and Mass Transfer* 41, 1998, pp. 3005 -3013.
[7] T.B. Gatski, M.Y. Hussaini and J.L. Lumley (1996) *Simulation and Modeling of Turbulent Flows*, New York, Oxford University Press.
[8] F.P. Incropera et al., *Introduction to Heat Transfer*, John Wiley&Sons, 2007.